ACS Energy LETTERS

Cite This: ACS Energy Lett. 2020, 5, 232−237

http://pubs.acs.org/journal/aelccp

LETTER

Integration of a Hydrogenase in a Lead Halide Perovskite Photoelectrode for Tandem Solar Water Splitting

Esther Edwardes Moore,[†] Virgil Andrei,[†] Sónia Zacarias,[‡] Inês A. C. Pereira,[‡] and Erwin Reisner*[,†]

[†]Department of Chemistry, University of Cambridge, Lensfield Road, Cambridge CB2 1EW, United Kingdom

[‡]Instituto de Tecnologia Química e Biológica António Xavier, Universidade Nova de Lisboa, Av. da Republica, 2780-157 Oeiras, Portugal

Supporting Information

ABSTRACT: **Lead halide perovskite solar cells are notoriously moisture-sensitive, but recent encapsulation strategies have demonstrated their potential application as photoelectrodes in aqueous solution. However, perovskite photoelectrodes rely on precious metal co-catalysts, and their combination with biological materials remains elusive in integrated devices. Here, we interface [NiFeSe] hydrogenase from *Desulfovibrio vulgaris* Hildenborough, a highly active enzyme for H_2 generation, with a triple cation mixed halide perovskite. The perovskite−hydrogenase photoelectrode produces a photocurrent of −5 mA cm^{-2} at 0 V vs RHE during AM1.5G irradiation, is stable for 12 h and the hydrogenase exhibits a turnover number of 1.9 × 10^6. The positive onset potential of +0.8 V vs RHE allows its combination with a $BiVO_4$ water oxidation photoanode to give a self-sustaining, bias-free photoelectrochemical tandem system for overall water splitting (solar-to-hydrogen efficiency of 1.1%). This work demonstrates the compatibility of immersed perovskite elements with biological catalysts to produce hybrid photoelectrodes with benchmark performance, which establishes their utility in semiartificial photosynthesis.**

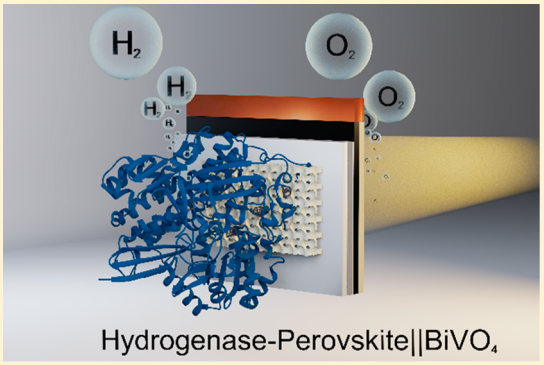

As a globally abundant and economical energy source, solar energy is the fastest growing renewable alternative to fossil fuels.[1,2] Artificial photosynthesis uses sunlight for the production of renewable chemical fuels, so-called solar fuels, thus addressing the intermittency limitations of photovoltaic (PV) technologies.[3,4] Solar fuel synthesis can be achieved by direct coupling of an efficient light absorber to a fuel-producing catalyst.[5,6] Organic−inorganic lead halide perovskites have received much attention due to their low production costs and promising PV cell efficiencies, currently reaching up to 25.2%.[2,7−10] However, moisture, air, and temperature instability has challenged the use of perovskites in photoelectrochemical (PEC) devices.[11,12] Encapsulation layers such as eutectic metal alloys, metal foils, and epoxy resin have improved the operation lifetime of solution-immersed perovskite-based photoelectrodes from seconds to hours.[11,13−17] However, all H_2-evolving PEC perovskite photocathodes have so far employed high-cost, low-abundance Pt nanoparticles as the co-catalyst.

Semiartificial photosynthesis combines the evolutionarily optimized activity of biological catalysts, such as isolated enzymes, with synthetic photoabsorbers.[18−21] Hydrogenases (H_2ases) are reversible and highly efficient H_2 production enzymes with a per-active-site activity matching that of Pt.[22−24] The integration of H_2ase with Si and Cu_2O photocathodes has previously been achieved,[25−29] but the combination with an immersed lead halide perovskite has remained inaccessible due to the moisture sensitivity of this photoabsorber and difficulty of achieving a productive enzyme−photoabsorber interface.

Here, a perovskite−H_2ase photocathode is presented, realized by an encapsulation system that protects the photoabsorber and provides a biocompatible, bespoke porous TiO_2 scaffold for the enzyme. This semiartificial photocathode enabled combination with a $BiVO_4$ water oxidation photoanode for bias-free, tandem PEC water splitting into H_2 and O_2 (Figure 1).

Optimized cesium formamidinium methylammonium (CsFAMA) triple cation mixed halide perovskite devices with a Field's metal (FM) protection layer were assembled and characterized as previously reported (Figure 1; see SI Experimental Procedures and Figure S1 for details).[15] Enzymes

Received: November 10, 2019
Accepted: December 10, 2019
Published: December 10, 2019

DOI: 10.1021/acsenergylett.9b02437
ACS Energy Lett. 2020, 5, 232−237

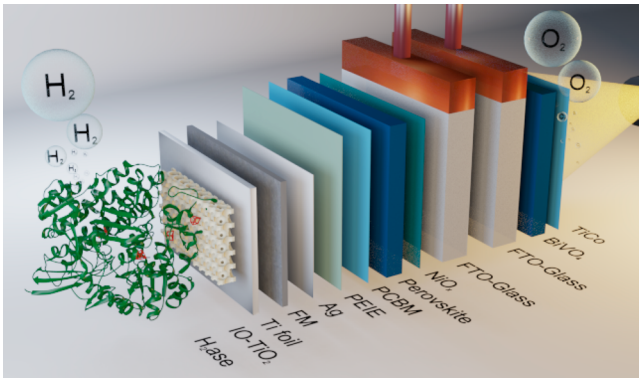

Figure 1. Schematic representation of the tandem PEC cell consisting of a FM-encapsulated perovskite photocathode with H_2ase integrated into an IO-TiO_2 layer and a $BiVO_4$ photoanode. TiCo refers to the water oxidation layer precursor: $[Ti_4O(OEt)_{15}(CoCl)]$. PCBM: [6,6]-phenyl-C_{61}-butyric acid methyl ester. PEIE: polyethylenimine.

have been integrated with high loading into hierarchically structured, macro- and mesoporous, inverse opal (IO) metal oxide scaffolds.[25,30,31] TiO_2 was selected in this study for its stability and conductivity under reducing conditions as well as its ability to form a biocompatible interface with enzymes.[25,32,33] The high-temperature (>100 °C) sensitivity of the perovskite prevented in situ annealing of the IO-TiO_2 directly on the FM surface. Therefore, anatase TiO_2 nanoparticles (~21 nm Ø) were first co-assembled with polystyrene beads (750 nm Ø) on Ti foil and annealed at 500 °C to give Ti|IO-TiO_2 (Figure S2). The geometrical surface area of the IO-TiO_2 scaffold was 0.28 cm^2 with an IO-TiO_2 film thickness of 15 μm. The Ti|IO-TiO_2 was then joined to the protected perovskite by briefly melting the FM sheet with a Peltier thermoelectric element (at ~70 °C), and an epoxy resin was used to seal the edges to give the encapsulated PV-integrated photocathode: PVK|IO-TiO_2 [FTO-glass|NiO_x|perovskite|PCBM|PEIE|Ag|FM|Ti|IO-TiO_2] (Figure 1).

A [NiFeSe] H_2ase from *Desulfovibrio vulgaris* Hildenborough (*Dv*H) was selected for its considerable H_2 evolution activity compared to that of *Dv*H [NiFe] H_2ase, and was purified and characterized as previously reported.[23,33−37] The selenocysteine residue (Sec489) in the active site (Figure S3) causes improved O_2 tolerance,[35,37−40] which is beneficial for its application in overall water splitting. The [NiFeSe] H_2ase (5 μL, 50 pmol) was drop-cast onto Ti|IO-TiO_2 and left to saturate the film for 30 min in a N_2 atmosphere. Protein film voltammetry of the Ti|IO-TiO_2|H_2ase electrode in a three-electrode configuration demonstrated that proton reduction occurred with minimal overpotential, indicative of efficient charge transfer at the TiO_2−H_2ase interface (Figure S4). The quality of the interface can be attributed to the well-known strength of protein binding to TiO_2, an effect that may be further accentuated by polarization of the TiO_2 surface.[25,33,41] The Ti|IO-TiO_2|H_2ase electrode displayed current densities of −2.5 mA cm^{-2} with high stability for several hours at an applied potential (E_{app}) of −0.5 V vs RHE under N_2, including some robustness in the presence of O_2. A Faradaic efficiency for H_2, FE_{H_2}, of 78% after 24 h was determined by gas chromatography. The E_{app} of −0.5 V vs RHE was applied to reflect the estimated perovskite photovoltage of 0.9 V in the PEC experiments, where +0.4 V vs RHE has been applied (see below).

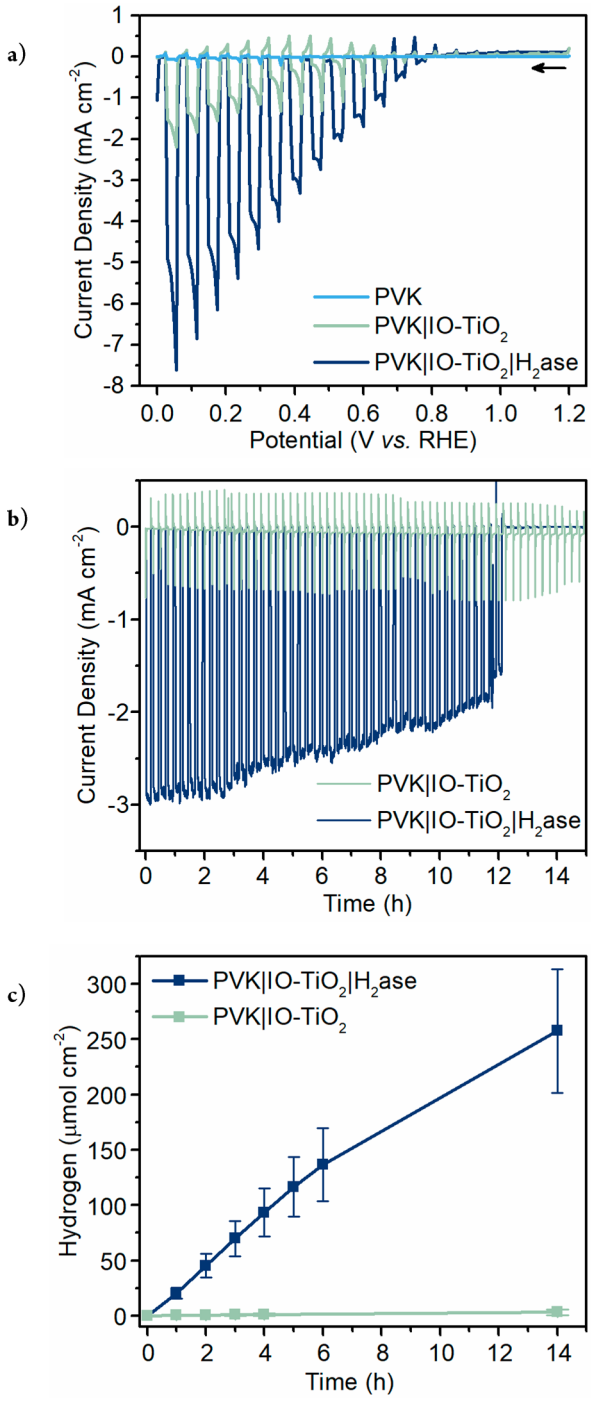

Figure 2. Photoelectrochemistry of a biohybrid photocathode. (a) Representative LSV of PVK|IO-TiO_2|H_2ase (blue), PVK|IO-TiO_2 (green), and PVK (light blue) electrodes with chopped illumination at a scan rate of 10 mV s^{-1}. Arrow indicates start of scan. (b) Representative CPPE at E_{app} = +0.4 V vs RHE, with a dark period lasting 5 min following every 10 min of light exposure. (c) Mean (N = 3) H_2 evolution from CPPE quantified by gas chromatography. Conditions: MES (50 mM, pH 6.0), KCl (50 mM), *Dv*H [NiFeSe] H_2ase (50 pmol), simulated solar light back-irradiation (AM1.5G, 100 mW cm^{-2}), N_2 atmosphere, 25 °C.

Protein−film photoelectrochemistry of the PVK|IO-TiO_2|H_2ase photocathode (three-electrode configuration, H_2ase

DOI: 10.1021/acsenergylett.9b02437
ACS Energy Lett. 2020, 5, 232−237

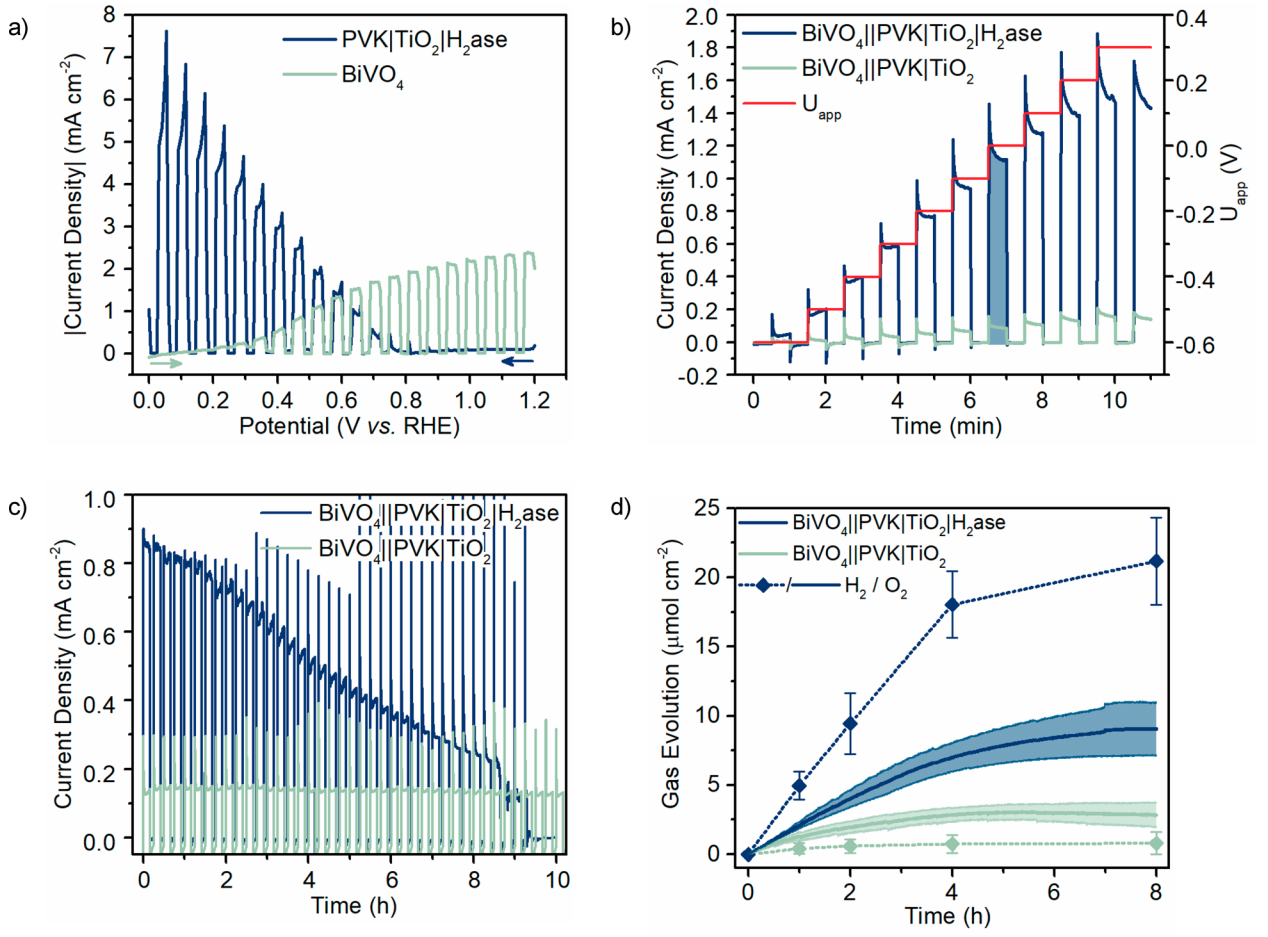

Figure 3. Photoelectrochemistry of the tandem device. (a) Representative LSV of PVK|TiO_2|H_2ase (blue) and $BiVO_4$ (green) electrodes with chopped illumination, forward scan, 10 mV s^{-1} scan rate, showing the absolute current densities. (b) Representative stepped potential chronoamperometry of $BiVO_4$||PVK|TiO_2|H_2ase (blue) and H_2ase-free $BiVO_4$||PVK|TiO_2 (green) tandem cells from U_{app} = −0.6 to +0.3 V. The current density at U_{app} = 0.0 V has been highlighted. (c) Representative CPPE of $BiVO_4$||PVK|TiO_2|H_2ase (blue) and H_2ase-free $BiVO_4$||PVK|TiO_2 (green) tandem cells at U_{app} = 0.0 V, with a dark period lasting 5 min following every 10 min of light exposure. (d) Mean (N = 3) H_2 (dotted line with measurement points) and O_2 (solid line) evolution from CPPE repeats. Conditions: MES (50 mM, pH 6.0), KCl (50 mM), *Dv*H [NiFeSe] H_2ase (50 pmol), simulated solar light irradiation (AM1.5G, 100 mW cm^{-2}), N_2 atmosphere, 25 °C.

integrated as above) was conducted at 25 °C under chopped simulated solar light irradiation (100 mW cm^{-2}, AM1.5G). The photocathode was irradiated from the back, which prevented photoexcitation of TiO_2. Linear sweep voltammetry (LSV) of the assembled PVK|IO-TiO_2|H_2ase electrode showed a cathodic onset potential at +0.8 V vs RHE and a photocurrent density of approximately −5 mA cm^{-2} at 0 V vs RHE (Figure 2a).

Controlled potential photoelectrolysis (CPPE) was conducted at +0.4 V vs RHE, and gas chromatography was used to quantify H_2 evolution yields. CPPE demonstrated the stability of the photocathode, which consistently achieved 12 h of catalysis (Figure 2b). Failure of the enzyme−photocathode after 12 h was likely due to water influx into the encapsulated perovskite, consistent with previous reports (Figure S5).[13,15] The stability of the equivalent PVK-Pt device was found to be comparable, supporting failure of the perovskite as the limit to longevity (Figure S6). The H_2ase electrode generated 258 ± 55 μmol_{H_2} cm^{-2} of H_2, whereas the enzyme-free electrode produced <1 μmol_{H_2} cm^{-2} (Figure 2c). The FE_{H_2} of PVK|IO-TiO_2|H_2ase after 14 h was (91 ± 1.5)% with a H_2ase-based turnover number (TON_{H_2}) of 1.9 × 10^6 and turnover frequency (TOF_{H_2}) of 95 s^{-1}.

Bias-free tandem water splitting has long been a desirable goal for PEC cells.[25,31,42,43] Here a $BiVO_4$-based water oxidation photoanode was prepared by electrodeposition of BiOI, then drop-casting and annealing a vanadium precursor, and finally spin-coating a layer of a cobalt-containing co-catalyst, as previously reported.[15,44] PEC analysis of the photoanode (three-electrode setup; Figure S7) gave an onset potential of +0.1 V vs RHE and a current density of 2.4 mA cm^{-2} at +1.23 V vs RHE.

The positive onset potential of the PVK|IO-TiO_2|H_2ase photocathode is essential for combination with the $BiVO_4$ photoanode to assemble a tandem water splitting PEC device. The $BiVO_4$ photoanode has been shown to absorb wavelengths below 500 nm and therefore limits the perovskite to absorption at 500−800 nm.[15] Nevertheless, the $BiVO_4$ photoanode remains the current-limiting absorber (Figure 3a). The robustness of the [NiFeSe] H_2ase towards O_2 (Figure S4) provided the possibility to assemble a "semiartificial leaf", where the photoelectrodes were not separated into two compartments by a membrane. The $BiVO_4$||PVK|TiO_2|H_2ase

DOI: 10.1021/acsenergylett.9b02437
ACS Energy Lett. 2020, 5, 232−237

Table 1. Solar-to-Fuel Efficiencies of State-of-the-Art Tandem Devices that Employ Immobilized Earth-Abundant Molecular H_2 Catalysts, a Bacterial Catalyst, and an Analogous Pt Device

System	Tandem Cell[a]	Solar-to-Fuel/%	Product	Ref
platinum	$BiVO_4$‖PVK|Pt	0.35	H_2	15
synthetic	Ru|OD|TiO_2‖NiO|OD|Co	0.05	H_2	42
	TaON|CoO_x‖$CuGaO_2$|OD|Co	0.0054	H_2	47
enzymatic	IO-TiO_2|OD|P_{Os}-PSII‖IO-ITO|H_2ase	0.14 (0.3 V bias)	H_2	31
	$BiVO_4$‖p-Si|IO-TiO_2|H_2ase	0.006	H_2	25
	$BiVO_4$‖PVK|IO-TiO_2|H_2ase	1.1	H_2	this work
bacterial	TiO_2‖Si|TiO_2|*S. Ovata*	0.38	acetate	48

[a]OD = organic dye. See Table S2 for details.

tandem cell (Figure 1) was prepared and PEC analysis undertaken in a single-compartment with illumination through the front of the $BiVO_4$ photoanode.

The two-electrode device achieved a current density of 1.1 mA cm^{-2} under bias-free conditions (U_{app} = 0.0 V), and stepped potential chronoamperometry revealed an onset potential of −0.6 V (Figure 3b). Bias-free CPPE showed a gradual decrease in photocurrent over 8 h, which was attributed to slowly progressing film loss due to enzyme inactivation, reorientation, or desorption (Figure 3c). In agreement, the current density returned to almost the initial value when a sacrificial electron acceptor (methyl viologen) was added to the tandem PEC cell after prolonged irradiation (Figure S8). The peak FE of the device was (82 ± 3)% for H_2 and (50 ± 8)% for O_2 (Figure 3d, FE over time; Figure S9). The lower FE for O_2 can be attributed to some O_2 reduction at the photocathode leading to lower amounts of O_2 detected. The solar-to-hydrogen efficiency (STH) was 1.1% (eq S1).

The $BiVO_4$‖PVK|TiO_2|H_2ase cell produced 21.2 ± 3.2 μmol_{H_2} cm^{-2} and 9.0 ± 2.7 μmol_{O_2} cm^{-2} after 8 h of CPPE, giving a H_2:O_2 ratio of 2.3. The PVK|IO-TiO_2|H_2ase photocathode (Figure S10) and $BiVO_4$‖PVK|TiO_2|H_2ase tandem device (Table 1, Figure S11) compare favorably with state-of-the-art H_2 production PEC systems employing earth-abundant molecular catalysts (synthetic and biological) in pH-benign aqueous solution (see Tables S1 and S2 for details). Semiartificial H_2 evolution photocathodes have been previously reported (Figure S10, color): a [NiFeSe] H_2ase from *Desulfomicrobium baculatum* was introduced onto a p-silicon (p-Si) photoabsorber via an IO-TiO_2 scaffold,[25] whereas [FeFe] H_2ases have been combined with both p-type CuO_2 and black-Si photoabsorbers.[26,27] Of the systems that employed small-molecule catalysts (Figure S10, gray scale), a Ni Dubois-type catalyst applied to a p-Si photoabsorber and Fe-porphyrin and polymeric Co-based catalysts combined with a GaP photocathode provide state-of-the-art performances.[28,45,46] Previously reported tandem earth-abundant molecular catalyzed PEC water splitting devices have utilized dye-sensitized p-type semiconductors with cobaloxime H_2 catalysts, resulting in STH values below 0.05% (Table 1).[42] A semiartificial tandem cell with a H_2ase cathode was wired to an organic dye−photosystem II photoanode, with a STH of 0.14% at 0.3 V applied bias.[31,47] However, the only previously reported H_2ase photocathode in a tandem cell employed a p-Si photoabsorber and achieved a STH of 0.006% for bias-free water splitting.[25] The unassisted solar-to-fuel conversion of the $BiVO_4$‖PVK|TiO_2|H_2ase tandem device was also more efficient than previous bacterial biohybrid systems.[48] The PVK-H_2ase system presented here shows superior performance to equivalent earth-abundant molecular artificial and biological catalyst systems reported to date.

In conclusion, the combination of a biocatalyst with a moisture-sensitive perovskite photoabsorber has been accomplished, and this biomaterial hybrid has subsequently been employed in overall tandem solar water splitting. The perovskite−H_2ase photocathode was realized by (i) encapsulating the perovskite using a eutectic alloy, metal foil, and epoxy resin and (ii) integrating the enzyme into a hierarchical IO-TiO_2 scaffold. The PVK|IO-TiO_2|H_2ase system achieved benchmark performance for photocathodes driven by earth-abundant catalysts with a current density of −5 mA cm^{-2} at 0.0 V vs RHE, a positive onset potential of +0.8 V vs RHE, a H_2 production yield of 258 ± 55 μmol_{H_2} cm^{-2} and a H_2ase-based TON_{H_2} of 1.9 × 10^6. A bias-free semiartificial water splitting device was produced using the PVK|IO-TiO_2|H_2ase photocathode and a water oxidizing $BiVO_4$ photoanode. In a single-compartment "leaf" configuration, the tandem PEC system was shown to have an onset potential of −0.6 V and a solar-to-hydrogen efficiency of 1.1% without applied bias. This work provides a new benchmark for photocathodes and tandem PEC devices employing earth-abundant molecular H_2 production catalysts. The hybrid system demonstrates the potential for bias-free fuel production and establishes perovskites as a suitable photoelectrode material for the integration of biological catalysts.

■ ASSOCIATED CONTENT

Supporting Information

The Supporting Information is available free of charge at https://pubs.acs.org/doi/10.1021/acsenergylett.9b02437.

Experimental procedures, photovoltaic parameters of perovskite cells, SEM of the IO-TiO_2 electrode, 3D representation of the [NiFeSe] H_2ase enzyme, protein film voltammetry of the Ti|IO-TiO_2|H_2ase electrode, photoelectrochemistry of the $BiVO_4$ photoanode, additional tandem device studies, performance comparison radar plots, and tables of state-of-the-art photocathodes and tandem devices (PDF)

■ AUTHOR INFORMATION

Corresponding Author

*E-mail: reisner@ch.cam.ac.uk.

ORCID

Erwin Reisner: 0000-0002-7781-1616

Author Contributions

E.E.M., V.A., and E.R. designed the project. E.E.M synthesized and characterized the IO-TiO_2 material, encapsulated the

DOI: 10.1021/acsenergylett.9b02437
ACS Energy Lett. 2020, 5, 232−237

devices, and carried out the electrochemistry and photoelectrochemistry. V.A. prepared and characterized the perovskite solar cells and the $BiVO_4$ photoanodes. S.Z. and I.A.C.P. expressed, purified, and characterized the *Dv*H [NiFeSe] hydrogenase. E.E.M., V.A., and E.R. analyzed the data. E.E.M. and E.R. wrote the manuscript with contributions and discussions from all authors. E.R. supervised the research work.

Notes

The authors declare no competing financial interest.

■ ACKNOWLEDGMENTS

This work was supported by an ERC Consolidator Grant "MatEnSAP" (682833; to E.E.M., E.R.) and the University of Cambridge (Vice-Chancellor and Winton scholarships to V.A.). Fundação para a Ciência e Tecnologia (Portugal) fellowship SFRH/BD/116515/2016, Grant PTDC/BBB-BEP/2885/2014, R&D units UID/Multi/04551/2013 (Green-IT) and LISBOA-01-0145-FEDER-007660 (MostMicro), co-funded by FCT/MCTES and FEDER funds through COMPETE2020/POCI, and European Union's Horizon 2020 research and innovation programme (GA 810856). We thank Prof Dominic S. Wright for a gift of the TiCo precatalyst.

■ REFERENCES

(1) Coyle, E. D.; Simmons, R. A. *Understanding the Global Energy Crisis*; Purdue University Press: Lafayette, March 2014.
(2) Nayak, P. K.; Mahesh, S.; Snaith, H. J.; Cahen, D. Photovoltaic solar cell technologies: analysing the state of the art. *Nat. Rev. Mater.* **2019**, *4*, 269.
(3) Tachibana, Y.; Vayssieres, L.; Durrant, J. R. Artificial photosynthesis for solar water-splitting. *Nat. Photonics* **2012**, *6*, 511−518.
(4) Dalle, K. E.; Warnan, J.; Leung, J. J.; Reuillard, B.; Karmel, I. S.; Reisner, E. Electro- and Solar-driven Fuel Synthesis with First Row Transition Metal Complexes. *Chem. Rev.* **2019**, *119* (4), 2752−2875.
(5) Jia, J.; Seitz, L. C.; Benck, J. D.; Huo, Y.; Chen, Y.; Ng, J. W. D.; Bilir, T.; Harris, J. S.; Jaramillo, T. F. Solar water splitting by photovoltaic-electrolysis with a solar-to-hydrogen efficiency over 30%. *Nat. Commun.* **2016**, *7*, 13237.
(6) Hisatomi, T.; Kubota, J.; Domen, K. Recent advances in semiconductors for photocatalytic and photoelectrochemical water splitting. *Chem. Soc. Rev.* **2014**, *43* (22), 7520−7535.
(7) National Renewable Energy Laboratory. https://www.nrel.gov/pv/assets/pdfs/best-research-cell-efficiencies.20191106.pdf (accessed 9 Nov 2019).
(8) Green, M. A.; Ho-Baillie, A.; Snaith, H. J. The emergence of perovskite solar cells. *Nat. Photonics* **2014**, *8*, 506−514.
(9) Jiang, Q.; Chu, Z.; Wang, P.; Yang, X.; Liu, H.; Wang, Y.; Yin, Z.; Wu, J.; Zhang, X.; You, J. Planar-Structure Perovskite Solar Cells with Efficiency beyond 21%. *Adv. Mater.* **2017**, *29*, 1703852.
(10) Kim, H.-S.; Hagfeldt, A.; Park, N.-G. Morphological and compositional progress in halide perovskite solar cells. *Chem. Commun.* **2019**, *55*, 1192−1200.
(11) Da, P.; Cha, M.; Sun, L.; Wu, Y.; Wang, Z. S.; Zheng, G. High-performance perovskite photoanode enabled by Ni passivation and catalysis. *Nano Lett.* **2015**, *15* (5), 3452−3457.
(12) Correa-Baena, J.-P.; Abate, A.; Saliba, M.; Tress, W.; Jacobsson, T. J.; Grätzel, M.; Hagfeldt, A. The rapid evolution of highly efficient perovskite solar cells. *Energy Environ. Sci.* **2017**, *10*, 710−727.
(13) Crespo-Quesada, M.; Pazos-Outón, L. M.; Warnan, J.; Kuehnel, M. F.; Friend, R. H.; Reisner, E. Metal-encapsulated organolead halide perovskite photocathode for solar-driven hydrogen evolution in water. *Nat. Commun.* **2016**, *7*, 12555.
(14) Zhang, H.; Yang, Z.; Yu, W.; Wang, H.; Ma, W.; Zong, X.; Li, C. A Sandwich-Like Organolead Halide Perovskite Photocathode for Efficient and Durable Photoelectrochemical Hydrogen Evolution in Water. *Adv. Energy Mater.* **2018**, *8*, 1800795.
(15) Andrei, V.; Hoye, R. L. Z.; Crespo-Quesada, M.; Bajada, M.; Ahmad, S.; De Volder, M.; Friend, R.; Reisner, E. Scalable Triple Cation Mixed Halide Perovskite−$BiVO_4$ Tandems for Bias-Free Water Splitting. *Adv. Energy Mater.* **2018**, *8*, 1801403.
(16) Poli, I.; Hintermair, U.; Regue, M.; Kumar, S.; Sackville, E. V.; Baker, J.; Watson, T. M.; Eslava, S.; Cameron, P. J. Graphite-protected $CsPbBr_3$ perovskite photoanodes functionalised with water oxidation catalyst for oxygen evolution in water. *Nat. Commun.* **2019**, *10*, 2097.
(17) Crespo-Quesada, M.; Reisner, E. Emerging approaches to stabilise photocorrodible electrodes and catalysts for solar fuel applications. *Energy Environ. Sci.* **2017**, *10*, 1116−1127.
(18) Kornienko, N.; Zhang, J. Z.; Sakimoto, K. K.; Yang, P.; Reisner, E. Interfacing nature's catalytic machinery with synthetic materials for semi-artificial photosynthesis. *Nat. Nanotechnol.* **2018**, *13*, 890−899.
(19) Evans, R. M.; Siritanaratkul, B.; Megarity, C. F.; Pandey, K.; Esterle, T. F.; Badiani, S.; Armstrong, F. A. The value of enzymes in solar fuels research − efficient electrocatalysts through evolution. *Chem. Soc. Rev.* **2019**, *48*, 2039−2052.
(20) Kim, J. H.; Nam, D. H.; Park, C. B. Nanobiocatalytic assemblies for artificial photosynthesis. *Curr. Opin. Biotechnol.* **2014**, *28*, 1−9.
(21) Lee, S. H.; Choi, D. S.; Kuk, S. K.; Park, C. B. Photobiocatalysis: Activating Redox Enzymes by Direct or Indirect Transfer of Photoinduced Electrons. *Angew. Chem., Int. Ed.* **2018**, *57* (27), 7958−7985.
(22) Tran, P. D.; Barber, J. Proton reduction to hydrogen in biological and chemical systems. *Phys. Chem. Chem. Phys.* **2012**, *14*, 13772−13784.
(23) Lubitz, W.; Ogata, H.; Rüdiger, O.; Reijerse, E. Hydrogenases. *Chem. Rev.* **2014**, *114*, 4081−4148.
(24) Jones, A. K.; Sillery, E.; Albracht, S. P. J.; Armstrong, F. A. Direct comparison of the electrocatalytic oxidation of hydrogen by an enzyme and a platinum catalyst. *Chem. Commun.* **2002**, 866−867.
(25) Nam, D. H.; Zhang, J. Z.; Andrei, V.; Kornienko, N.; Heidary, N.; Wagner, A.; Nakanishi, K.; Sokol, K. P.; Slater, B.; Zebger, I.; Hofmann, S.; Fontecilla-Camps, J. C.; Park, C. B.; Reisner, E. Solar Water Splitting with a Hydrogenase Integrated in Photoelectrochemical Tandem Cells. *Angew. Chem., Int. Ed.* **2018**, *57*, 10595−10599.
(26) Zhao, Y.; Anderson, N. C.; Ratzloff, M. W.; Mulder, D. W.; Zhu, K.; Turner, J. A.; Neale, N. R.; King, P. W.; Branz, H. M. Proton Reduction Using a Hydrogenase-Modified Nanoporous Black Silicon Photoelectrode. *ACS Appl. Mater. Interfaces* **2016**, *8* (23), 14481−14487.
(27) Tian, L.; Németh, B.; Berggren, G.; Tian, H. Hydrogen evolution by a photoelectrochemical cell based on a Cu_2O-ZnO-[FeFe] hydrogenase electrode. *J. Photochem. Photobiol., A* **2018**, *366*, 27−33.
(28) Leung, J. J.; Warnan, J.; Nam, D. H.; Zhang, J. Z.; Willkomm, J.; Reisner, E. Photoelectrocatalytic H_2 evolution in water with molecular catalysts immobilised on p-Si *via* a stabilising mesoporous TiO_2 interlayer. *Chem. Sci.* **2017**, *8*, 5172−5180.
(29) Lee, C. Y.; Park, H. S.; Fontecilla-Camps, J. C.; Reisner, E. Photoelectrochemical H_2 Evolution with a Hydrogenase Immobilized on a TiO_2-Protected Silicon Electrode. *Angew. Chem., Int. Ed.* **2016**, *55* (20), 5971−5974.
(30) Mersch, D.; Lee, C.-Y.; Zhang, J. Z.; Brinkert, K.; Fontecilla-Camps, J. C.; Rutherford, A. W.; Reisner, E. Wiring of Photosystem II to Hydrogenase for Photoelectrochemical Water Splitting. *J. Am. Chem. Soc.* **2015**, *137*, 8541−8549.
(31) Sokol, K. P.; Robinson, W. E.; Warnan, J.; Kornienko, N.; Nowaczyk, M. M.; Ruff, A.; Zhang, J. Z.; Reisner, E. Bias-free photoelectrochemical water splitting with photosystem II on a dye-sensitized photoanode wired to hydrogenase. *Nat. Energy* **2018**, *3*, 944−951.
(32) Miller, M.; Robinson, W. E.; Oliveira, A. R.; Heidary, N.; Kornienko, N.; Warnan, J.; Pereira, I. A. C.; Reisner, E. Interfacing Formate Dehydrogenase with Metal Oxides for the Reversible Electrocatalysis and Solar-Driven Reduction of Carbon Dioxide. *Angew. Chem., Int. Ed.* **2019**, *58* (14), 4601−4605.

DOI: 10.1021/acsenergylett.9b02437
ACS Energy Lett. 2020, 5, 232−237

(33) Wombwell, C.; Caputo, C. A.; Reisner, E. [NiFeSe]-Hydrogenase Chemistry. *Acc. Chem. Res.* **2015**, *48*, 2858−2865.
(34) Zacarias, S.; Vélez, M.; Pita, M.; De Lacey, A. L.; Matias, P. M.; Pereira, I. A. C. Characterization of the [NiFeSe] hydrogenase from *Desulfovibrio vulgaris* Hildenborough. *Methods Enzymol.* **2018**, *613*, 169−201.
(35) Gutierrez-Sanchez, C.; Rudiger, O.; Fernandez, V. M.; De Lacey, A. L.; Marques, M.; Pereira, I. A. Interaction of the active site of the Ni-Fe-Se hydrogenase from *Desulfovibrio vulgaris* Hildenborough with carbon monoxide and oxygen inhibitors. *JBIC, J. Biol. Inorg. Chem.* **2010**, *15* (8), 1285−1292.
(36) Valente, F. M. A.; Oliveira, A. S. F.; Gnadt, N.; Pacheco, I.; Coelho, A. V.; Xavier, A. V.; Teixeira, M.; Soares, C. M.; Pereira, I. A. C. Hydrogenases in *Desulfovibrio vulgaris* Hildenborough: structural and physiologic characterisation of the membrane-bound [NiFeSe] hydrogenase. *JBIC, J. Biol. Inorg. Chem.* **2005**, *10* (6), 667−682.
(37) Marques, M. C.; Tapia, C.; Gutiérrez-Sanz, O.; Ramos, A. R.; Keller, K. L.; Wall, J. D.; De Lacey, A. L.; Matias, P. M.; Pereira, I. A. C. The direct role of selenocysteine in [NiFeSe] hydrogenase maturation and catalysis. *Nat. Chem. Biol.* **2017**, *13*, 544−550.
(38) Marques, M. C.; Coelho, R.; De Lacey, A. L.; Pereira, I. A.; Matias, P. M. The three-dimensional structure of [NiFeSe] hydrogenase from *Desulfovibrio vulgaris* Hildenborough: a hydrogenase without a bridging ligand in the active site in its oxidised, "as-isolated" state. *J. Mol. Biol.* **2010**, *396* (4), 893−907.
(39) De Lacey, A. L.; Gutierrez-Sanchez, C.; Fernandez, V. M.; Pacheco, I.; Pereira, I. A. FTIR spectroelectrochemical characterization of the Ni-Fe-Se hydrogenase from *Desulfovibrio vulgaris* Hildenborough. *JBIC, J. Biol. Inorg. Chem.* **2008**, *13* (8), 1315−1320.
(40) Parkin, A.; Goldet, G.; Cavazza, C.; Fontecilla-Camps, J. C.; Armstrong, F. A. The Difference a Se Makes? Oxygen-Tolerant Hydrogen Production by the [NiFeSe]-Hydrogenase from *Desulfomicrobium baculatum*. *J. Am. Chem. Soc.* **2008**, *130* (40), 13410−13416.
(41) Leader, A.; Mandler, D.; Reches, M. The role of hydrophobic, aromatic and electrostatic interactions between amino acid residues and a titanium dioxide surface. *Phys. Chem. Chem. Phys.* **2018**, *20*, 29811−29816.
(42) Li, F.; Fan, K.; Xu, B.; Gabrielsson, E.; Daniel, Q.; Li, L.; Sun, L. Organic Dye-Sensitized Tandem Photoelectrochemical Cell for Light Driven Total Water Splitting. *J. Am. Chem. Soc.* **2015**, *137*, 9153−9159.
(43) Zhang, K.; Ma, M.; Li, P.; Wang, D. H.; Park, J. H. Water Splitting Progress in Tandem Devices: Moving Photolysis beyond Electrolysis. *Adv. Energy Mater.* **2016**, *6* (15), 1600602.
(44) Lai, Y. H.; Palm, D. W.; Reisner, E. Multifunctional Coatings from Scalable Single Source Precursor Chemistry in Tandem Photoelectrochemical Water Splitting. *Adv. Energy Mater.* **2015**, *5* (24), 1501668.
(45) Khusnutdinova, D.; Beiler, A. M.; Wadsworth, B. L.; Jacob, S. I.; Moore, G. F. Metalloporphyrin-modified semiconductors for solar fuel production. *Chem. Sci.* **2017**, *8*, 253−259.
(46) Beiler, A. M.; Khusnutdinova, D.; Wadsworth, B. L.; Moore, G. F. Cobalt Porphyrin−Polypyridyl Surface Coatings for Photoelectrosynthetic Hydrogen Production. *Inorg. Chem.* **2017**, *56* (20), 12178−12185.
(47) Windle, C.; Kumagai, H.; Higashi, M.; Brisse, R.; Bold, S.; Jousselme, B.; Chavarot-Kerlidou, M.; Maeda, K.; Abe, R.; Ishitani, O.; Artero, V. Earth-Abundant Molecular Z-Scheme Photoelectrochemical Cell for Overall Water-Splitting. *J. Am. Chem. Soc.* **2019**, *141* (24), 9593−9602.
(48) Liu, C.; Gallagher, J. J.; Sakimoto, K. K.; Nichols, E. M.; Chang, C. J.; Chang, M. C. Y.; Yang, P. Nanowire−Bacteria Hybrids for Unassisted Solar Carbon Dioxide Fixation to Value-Added Chemicals. *Nano Lett.* **2015**, *15*, 3634−3639.

DOI: 10.1021/acsenergylett.9b02437
ACS Energy Lett. 2020, 5, 232−237